Journal of Catalysis **184,** 335–348 (1999)
Article ID jcat.1999.2471, available online at http://www.idealibrary.com on IDEAL®

An Experimental Verification of the Physical Nature of Pt Adsorption onto Alumina

J. R. Regalbuto,[1] A. Navada, S. Shadid, M. L. Bricker,* and Q. Chen*

*Department of Chemical Engineering, University of Illinois at Chicago, 810 S. Clinton, Chicago, Illinois 60607; and *UOP Research Center, 50 E. Algonquin Road, Des Plaines, Illinois 60017*

Received September 3, 1998; revised March 8, 1999; accepted March 11, 1999

In the past decade increasing attention has been paid to catalyst preparation, and in particular to the impregnation step. Various models have been employed to describe the uptake of dissolved metal complexes by oxide surfaces as occurs in catalyst impregnation. These models include "coordination chemistry" models, "chemical adsorption" models, and "physical adsorption" models. In this paper, an experimental discrimination between these models is undertaken. The comprehensive body of experimental evidence presented here suggests that the mechanism for adsorption of Pt complexes arising from chloroplatinic acid onto alumina, under the normal impregnation conditions of room temperature and short (1 h) contact times, is purely physical. That Pt uptake does not depend on Al solubility implies that the coordinative mechanism is not operative. That adsorption of Cl^- is not the cause of Pt retardation at low pH contradicts the chemical mechanism of earlier models given for Pt adsorption onto alumina. All experimental data, including large pH shifts, are accounted for by a physical adsorption model which includes a realistic model of surface charging and a balance to account for proton transfer between the liquid and the surface. Since all aluminas have about the same PZC and charging parameters, they behave in an identical fashion regarding the uptake of Pt. All uptake-pH data, for the same amount of alumina surface, can be simulated for all aluminas using one theoretical revised physical adsorption (RPA) curve with no adjustable parameters.

Key Words: **Pt; alumina; adsorption; chemical adsorption; physical adsorption; catalyst impregnation; noble metal catalyst preparation.**

INTRODUCTION

In the last decade increasing attention has been paid to catalyst preparation, and in particular to the impregnation step. Owing to its relevance to industrial catalysis, noble metal impregnation onto alumina has been the subject of a good number of fundamental studies (1–12), including the classic series of Heise and Schwarz (1–4), the comprehensive and semiquantitative study of Contescu and Vass (6), and a number of more recent studies of Pt/alumina (7–12).

A schematic of the impregnation system as depicted in most recent adsorption studies is shown in Fig. 1. Three regimes have been delineated; in the first, the speciation of the coordination complexes of the noble metal must be modeled as a function of pH. This is performed easily enough if the solubility constants of all species are known. The second regime is the oxide surface. Hydroxyl groups populate oxide surfaces with densities in the range 5–20 OH/nm^2 (14). These groups are normally modeled as amphoteric species, becoming protonated and positively charged at low pH, and deprotonated and negatively charged at high pH (15). At the point of zero charge (PZC) the surface is neutral. The regime which distinguishes most models is the third, which contains the calculation of adsorption equilibrium constants between the metal complexes and the oxide surface.

The features that must be explained by an impregnation model can be surmised from the well-documented characteristics of Pt uptake over alumina as a function of pH (3, 9, 10, 12). Adsorption is minimal at the PZC of alumina, which for pure alumina surfaces is in the range 8–9 (14, 16). With anionic Pt complexes in solution such as $PtCl_6^{-2}$, evolved from chloroplatinic acid (CPA), uptake increases as pH falls from the PZC as the hydroxyl groups become protonated and so positively charged. However, even while the alumina surface remains fully charged, Pt uptake falls precipitously below a pH of about 3 (3, 7, 9, 10, 12). Adsorption models must account for this retardation at low pH. Secondly, the more complete measurements of impregnation have recorded drastic shifts in solution pH as the metal-containing solutions are contacted with the oxide (6, 7, 12, 17). These must also be accounted for.

Various models have been employed to describe the uptake of dissolved metal complexes by oxide surfaces as occurs in catalyst impregnation. These models include "coordination chemistry" models, proposed for hydrotalcite-forming materials such as Ni-Al_2O_3 (18), and are echoed in several studies of Pt-Al_2O_3 (13, 19). According to this

[1] To whom correspondence should be addressed. Fax: (312) 996-0808. E-mail: jrr@uic.edu.

0021-9517/99 $30.00

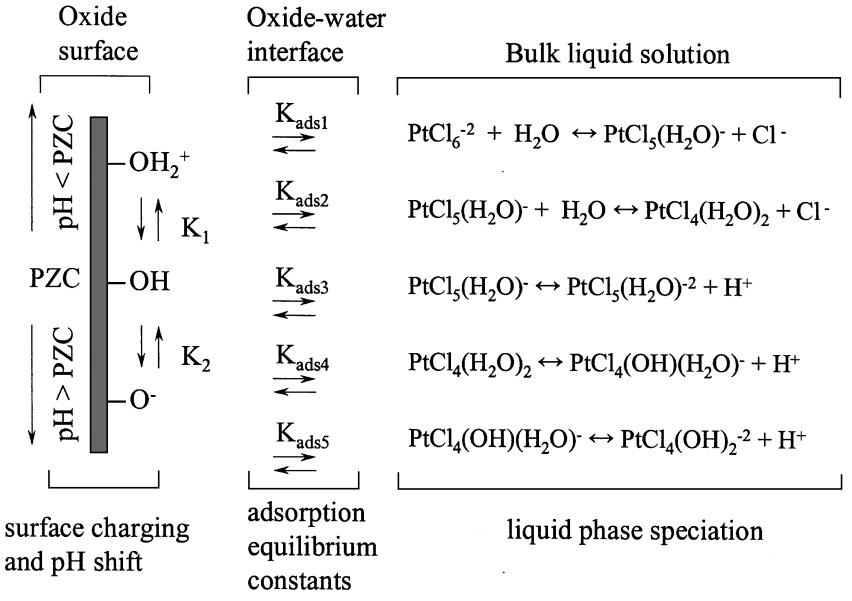

FIG. 1. The three regimes of an adsorption model.

hypothesis, adsorption of the hexachloroplatinate anion $PtCl_6^{-2}$ can proceed only subsequent to complexation with dissolved aluminum.

Quantitative adsorption models pertaining to catalyst impregnation have been employed and developed by several groups (7, 20), particularly the triple-layer modeling work of Lycourghiotis (20 and references within). These parameter-laden models are primarily based on "chemical" interactions between metal complexes and oxide surfaces. Fits to data are accomplished by adjusting the values of the adsorption equilibrium constants of the presumed "chemical interaction" steps of a mechanism. In this paper, "triple-layer" and "surface complexation" models based on this sort of presumed interaction are grouped together as "chemical" models.

One of the earliest adsorption models is that of James and Healy (21), who proposed that the adsorption of hydrolyzable metal cations was largely a physical process, capable of being described by an a priori calculation of coulombic and solvation contributions to the adsorption free energy. Indeed, early qualitative studies of noble metal adsorption onto alumina and/or silica suggest that the principal attraction is electrostatic (1, 6, 22). Positively charged oxide surfaces (at pH < PZC) are capable of adsorbing anions, and negatively charged surfaces (pH > PZC) are capable of adsorbing cations (22).

In practice, the original physical adsorption model contained an adjustable term as a correction for an admitted overestimate of the solvation energy that was loosely called a "chemical" interaction (21). That the magnitude of this adjustable term was so large may explain the eventual abandonment of this model (23).

Our work has centered on revising (23) and experimentally verifying the original model of James and Healy. In this paper we present principally an experimental discrimination between the various proposed models, the "coordinative chemical" model, the "chemical adsorption" models, and the "revised physical adsorption" (RPA) model as they pertain to the adsorption of Pt complexes from CPA over alumina. To explore the validity of the coordinative chemical theory, aluminas of different solubility have been used. If the adsorption mechanism is coordinative, the more soluble aluminas should adsorb more Pt. To investigate the fitness of the proposed chemical adsorption mechanisms, direct measurement of Cl^- uptake, a key feature of the chemical theories applied to Pt/alumina, is made. If the postulated chemical mechanisms are correct, the retardation of Pt adsorption at low pH will be accompanied by a commensurate uptake of Cl^- (7, 9).

The comprehensive body of experimental evidence presented here suggests that the mechanism of adsorption under the normal impregnation conditions of room temperature and short (1 h) contact times is not coordinative or chemical, but purely physical. Thus, since all aluminas have about the same PZC and charging parameters, they behave in an identical fashion regarding the uptake of Pt. All uptake-pH data, for the same amount of alumina surface, can be simulated for all aluminas using one theoretical RPA curve with no adjustable parameters.

EXPERIMENTAL

Aluminas of different phase (alpha, gamma, theta, and eta) and surface area (28–188 m^2/gm) were used and will be

TABLE 1

Alumina Properties

Sample name, phase	BET surface area (m^2/g)	Pore volume cm^3/g	PZC
Alpha 28	28	—	8.8
Alpha 32	32	0.109	8.4
Alpha 89	89	0.139	8.9
Alpha 130	130	0.170	9.2
Gamma 71	71	—	8.8
Gamma 147	147	—	8.8
Gamma 188	188	0.482	8.8
Theta 77	77	—	8.6
Eta 180[a]	180	0.265	9.4

[a] Contains 0.45 wt% Na impurity β.

identified in figure legends by phase and surface area, for example, "gamma 147" or "alpha 28." The characteristics of these aluminas are summarized in Table 1. The series of high surface area alpha aluminas was prepared by relatively low temperature (500°C) calcinations of diaspore. The PZC of each sample was obtained by the measurement of equilibrium pH at high oxide loading (EpHL) (17); the results are shown in Fig. 2. All of these alumina samples had PZC values in the range 8.4–9.4. A value of 8.5 was used for the RPA model calculations.

In adsorption experiments, the surface loading, or oxide area per liter of solution, was adjusted to the same value (500 m^2/L) for all experiments by adding different masses of oxide. Fifty milliliters of dilute CPA (close to 180 ppm Pt or 9.2×10^{-4} M), adjusted to various pH values using HCl or NaOH, was added to oxide powders previously weighed into polypropylene bottles. The amount of Pt in solution corresponded to about 10% excess of 1.6 μmol Pt/m^2, believed to be the maximum coverage for anionic Pt (15). The bottles were placed on a rotary shaker and intermittently sampled for pH and for Cl^- concentration with careful use of a Cl^- ion-specific electrode. At 1 or 24 h, 3- to 4-ml portions of the well-mixed suspensions were removed from the bottles and the solid was filtered to permit measurement of Pt and Al concentrations in the liquid phase by ICP. Adsorption density is calculated as the initial minus final concentration of Pt divided by the surface loading, and is expressed as micromoles Pt adsorbed per square meter.

The different solubility of the various aluminas (alpha is sparingly soluble, gamma is relatively highly soluble in acid solutions) permits an examination of the dependence of Pt adsorption on dissolved alumina. Aluminum

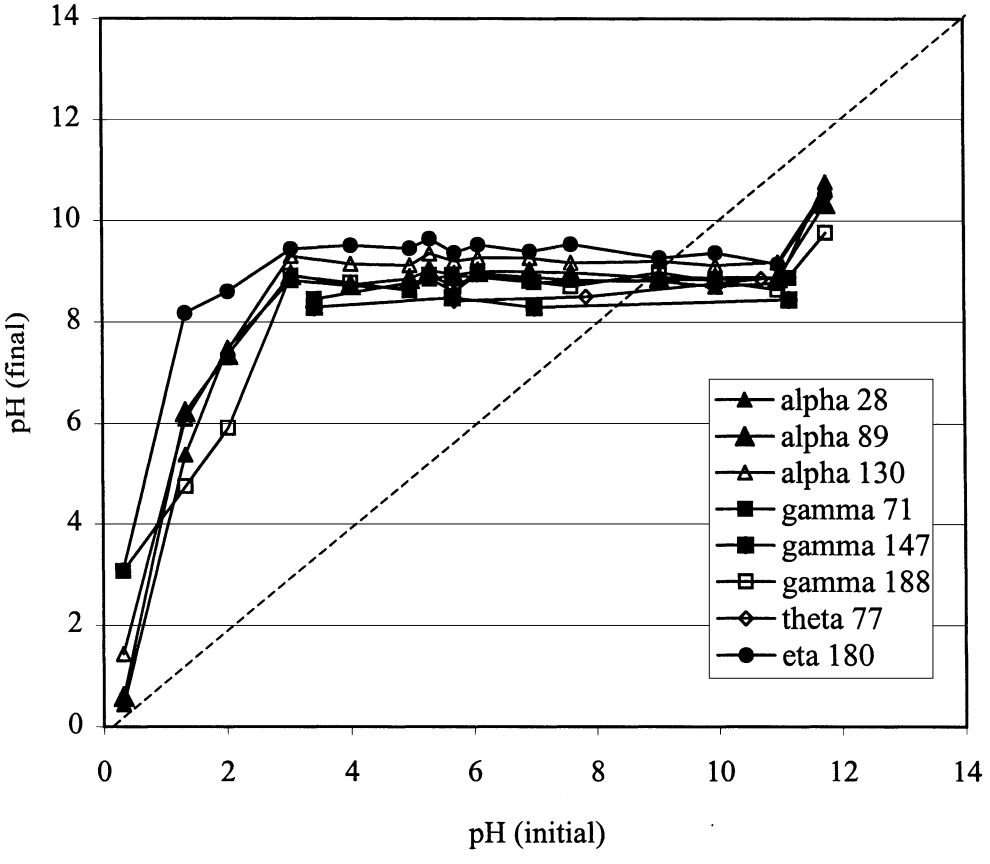

FIG. 2. EpHL measurement of alumina PZCs.

concentration was also measured by ICP. Chloride adsorption, a key component of the chemical adsorption mechanism, was also directly measured.

RESULTS

Preliminary Controls

Prior to the Pt/Al_2O_3 adsorption experiments, two controls were performed. In the first, CPA solutions were monitored in the absence of oxide, and in the second, the various oxides were monitored in the absence of CPA.

In the first control, CPA solutions were measured for Pt solubility, pH shifts, and changes in Cl^- concentration as the solutions were brought to various pH values. Data for this run are shown in Fig. 3. The initial target CPA solution was 180 ppm (9.2×10^{-4} mol Pt/L), which was diluted from a concentrated (0.2 M) stock CPA solution. The pH of this solution just after dilution was 2.73, which agrees closely with the value expected from complete dissociation of both hydrogens from CPA. Over a 1-week period, the pH of this 180 ppm solution shifted down to 2.53. To this aged solution, HCl was added to lower pH and NaOH was added to increase pH. The Pt concentrations measured 1 or 24 h after the solution preparations were equivalent and are shown in Fig. 3a.

While Pt levels were relatively constant throughout the pH range and independent of times up to a day or two, pH values (Fig. 3b) shifted markedly. In the central pH range (6–9) a decrease in pH occurred so quickly that the theoretical target pH values were never actually attained. Rapid shifts also occurred in Pt-free solutions in this pH range (seen as the lighter curve of Fig. 3b). Experiments with a glove box confirmed that the majority of the pH shifts in the range 7–9 were from CO_2 absorption; a glove box was not utilized in general, however, for a more realistic preparation procedure. The pH continued to shift significantly even outside of the range of CO_2 absorption. The 24-h readings in the 3–6 and 9–10 initial pH ranges were considerably below the 1-h readings. Substantial shifts continued at 48 h (not shown).

The amount of Cl^- released from the initial $PtCl_6^{-2}$ solution, starting at pH 2.5 and moving upward (where NaOH was added to increase pH), is shown in Fig. 3c. The initial solution itself contained 94 ppm of Cl^-; this was assumed to be in excess and was subtracted from the readings at higher pH values. The Cl^- evolution displays a first maximum at an initial pH of about 3.5, and a second at the highest initial pH of 11.

After several weeks of storage, Pt precipitates were observed for initial pH values in the central pH range (6–9). This occurred both in CPA solutions which had never been contacted with oxide and in solutions which had been contacted with oxide and filtered.

In the second set of control experiments, pH shifts, the disappearance of Cl^- from acid solutions, and the amount of dissolved alumina were measured for the various supports placed in acid and base solutions containing no CPA. Results of pH shifts at 1 h are shown in Fig. 4a and at 24 h in Fig. 4b. All these aluminas follow same trend; pH shifts up at low pH (below the PZCs of the aluminas) and down at high pH (above the PZCs). A shoulder at low pH is seen, especially pronounced at 24 h. This is associated with aluminum dissolution and will be discussed immediately below. Apart from this region, pH equilibrates more rapidly over the oxides than CPA-only solutions (Fig. 3b).

Solubilized aluminum from acidic and basic solutions is shown in Fig. 5a for representative samples at 24 h. The order of alumina solubility is alpha < theta, eta < gamma. As mentioned above, aluminum dissolution is manifested in the pH shifts of Fig. 4; shoulders at low pH grow in proportion to Al dissolved. Three protons are consumed for every Al dissolved (24) according to

$$Al_2O_3 + 6H^+ = 2Al^{+3} + 3H_2O.$$

As the low pH shoulders grow significantly from 1 to 24 h, so also the aluminum concentration greatly increases during this time.

Chloride data at 24 h are plotted in Fig. 5b as initial minus final concentration (or Cl^- disappearance). The disappearance of Cl^- from solution appears to be related to Al solubility: more Cl^- disappeared from the most soluble aluminas. This finding suggests that the Cl^- may not be adsorbed by these alumina surfaces, but reacts with the dissolved aluminum cations. The ratio of (Cl^- disappeared/Al dissolved) is plotted in Fig. 5c; the ratio of 3 at the lowest pH is observed for all samples with the exception of alpha 89. The curve for alpha 89 does not coincide with the others possibly due to the very low levels of Cl^- and dissolved Al for this sample, and a high degree of experimental uncertainty. The data suggest the formation of $AlCl_3$ precipitates. X-ray diffraction analysis was performed on gamma alumina samples that had been treated with concentrated HCl and dried; the $AlCl_3$ phase was indeed seen. The change in Cl^- concentration at low pH therefore appears to be caused primarily by complexation with dissolved Al.

CPA Adsorption onto Aluminas

Adsorption experiments consisted of monitoring Pt, dissolved Al, consumed or evolved Cl^-, and the shift in pH as CPA was added to various oxides at different pH values. The Pt concentration of 180 ppm (9.2×10^{-4} M) corresponds to about a 10% excess of one monolayer of Pt (1.6 μmol/m^2 (11)) for a surface loading of 500 m^2/L. Platinum uptake (in μmol/m^2) for different times is shown in Fig. 6. At both 1 h (Fig. 6a) and 24 h (Fig. 6b) the uptake of Pt is similar for all alumina samples and shows a volcano-type curve with a

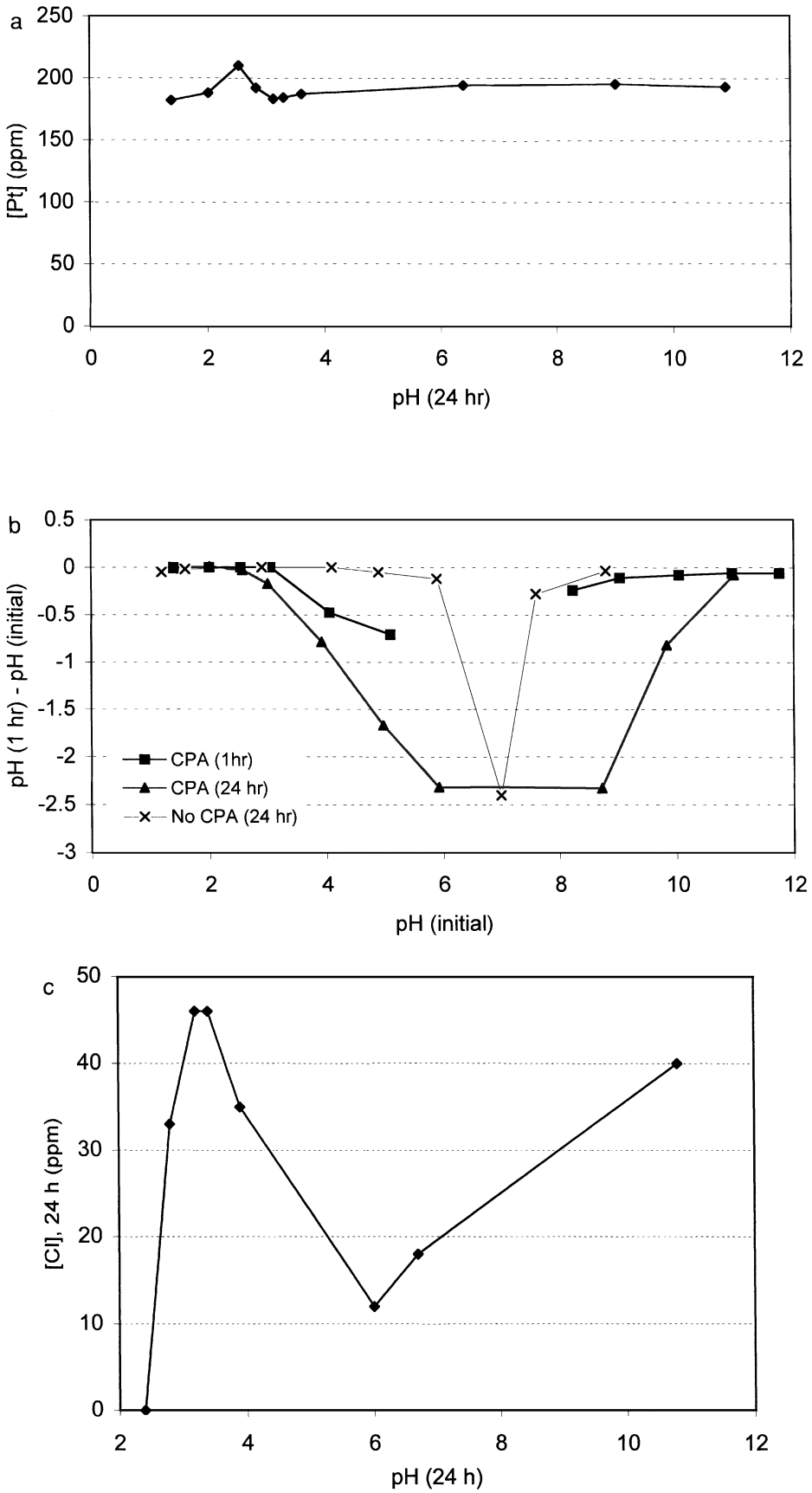

FIG. 3. Aqueous solutions of CPA (no oxide). (a) Pt concentration versus pH, (b) pH shifts versus $pH_{initial}$, and (c) Cl^- release versus pH.

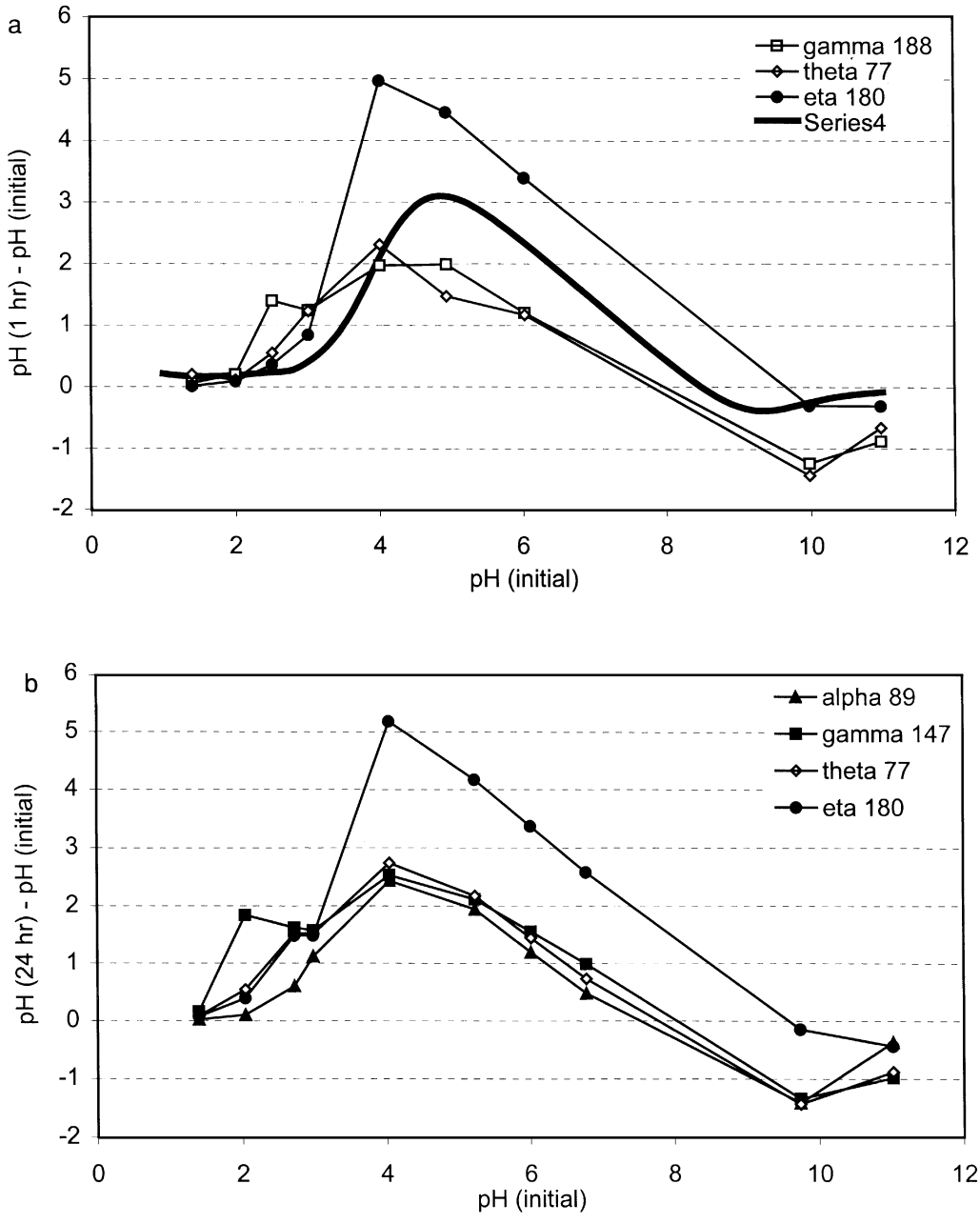

FIG. 4. Oxide-water mixtures (no CPA). pH shift versus $pH_{initial}$ at (a) 1 h (solid line is for RPA model) and (b) 24 h.

maximum at about pH 4. Similar curves have been seen by other groups (3, 7, 9). There is a great deal of scatter in the pH range 5–7 for the 1-h results. The difference between 1 and 24 h is seen in the middle pH range, where deposition of Pt has continued at long times and all samples show high uptake of Pt. At 24 h, there is even appreciable uptake at the oxides' PZCs, pH 8–9.

The pH shifts which correspond to the Pt adsorption data are shown in Fig. 7; at 1 h in Fig. 7a, and at 24 h in Fig. 7b. The pH shifts caused by the oxides are, like the control experiments, relatively rapid. At 24 h the shoulder at low pH (2–3.5) due to the dissolution of Al is again prominent. In general, the pH shifts appear similar to the Pt-free control experiment (Fig. 4).

Aluminum concentration versus pH is shown at 1 and 24 h in Figs. 8a and 8b. Compared to Pt adsorption (Figs. 6a and 6b), and the shifts in pH (Figs. 7a and 7b) the dissolution of Al is relatively slow. The continued dissolution of Al at long times is reflected in the pH shifts of Fig. 7b. The relative solubility of the aluminas is seen in Fig. 8 and agrees

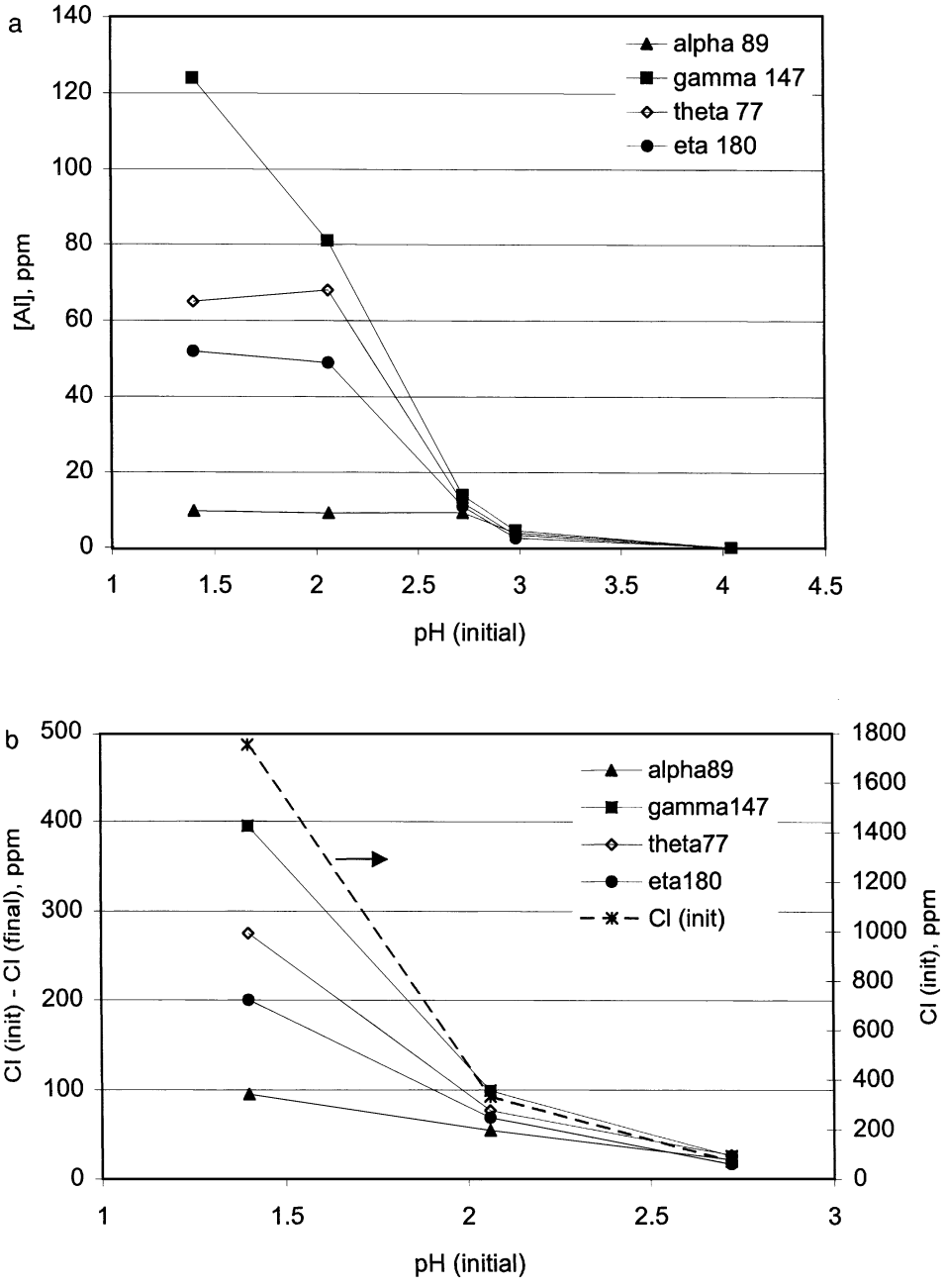

FIG. 5. Oxide-water mixtures (no CPA). (a) Dissolved Al, (b) Cl^- uptake, and (c) Cl^-/Al ratios versus $pH_{initial}$.

with the literature (24). The order, from most to least soluble, is gamma > theta, eta > alpha. The great difference in their solubility is not reflected by a difference in Pt uptake, however (Fig. 6).

The change in chloride concentration at 24 h (the only measurement made) in the low pH range and the amounts of Cl^- added to the solution as HCl are shown in Fig. 9. In this low pH range it appears that little or no Cl^- adsorption occurred, even while the Pt adsorption drops precipitously (Fig. 6).

DISCUSSION

Pt Speciation

Two sets of speciation data appear in the literature. Knozinger's group (7) employs a speciation diagram based on the speciation constants of Davidson and Jameson (25) and Cox and Peters (26). In that model, the diprotic CPA does not fully dissociate, and singly valent species of $HPtCl_5^-$ and $PtCl_5(H_2O)^-$ predominate in the low pH range (7). In the present work, the pH of CPA solutions always

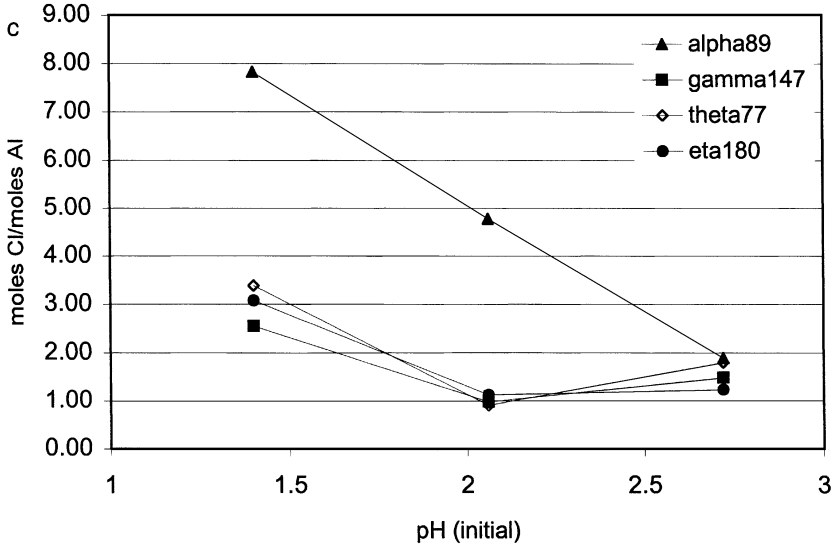

FIG. 5—*Continued*

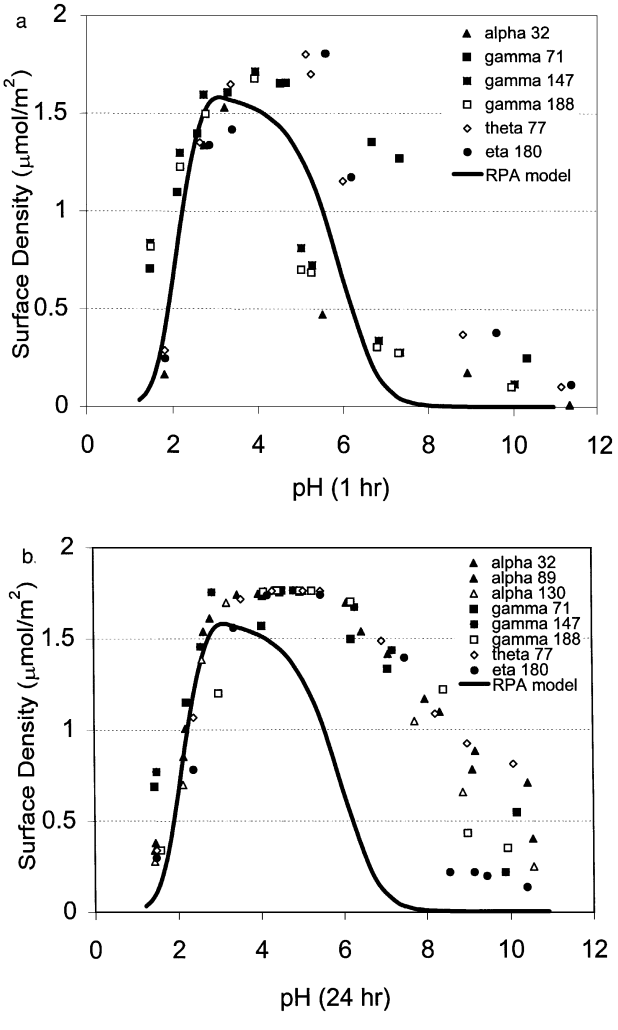

FIG. 6. Pt uptake by various aluminas versus pH at (a) 1 h and (b) 24 h. Solid lines are RPA model calculations.

corresponded to complete dissociation, even for concentrations of 0.20 M (which gave pH values of 0.38). More consistent with these observations is a set of speciation constants found in the reference text of Sillen and Martell (27). The resulting speciation diagram is shown in Fig. 10a and predicts the persistence of $PtCl_6^{-2}$ at low pH up through pH values of about 5, whereafter it is replaced by the similarly sized and doubly valent $PtCl_5(OH)^{-2}$. At high pH, the doubly valent $PtCl_4(OH)_2^{-2}$ species is predicted. There is some discrepancy between the experimental measurements of the CPA-only solutions (first control, Fig. 3) and this mechanism, however. In Fig. 10b the released Cl^-/Pt ratio calculated from Fig. 10a is compared to the measured (released Cl^-/Pt) ratio, taken from Fig. 3c. While both curves approach a ratio of 2 at high pH, corresponding to the formation of complexes comprised in part by $PtCl_4$, there is an unexpected maximum in the experimental points near pH 3. Also shown in Fig. 10b is the (H^+ evolved/Pt) ratios, which are calculated from the pH shifts of the CPA-only solutions in Fig. 3b. The number of protons released to solution is not sufficient to balance the release of Cl^-; it therefore appears that Cl^- was not wholly substituted by $(OH)^-$ as shown in Fig. 10a, but instead, species of lower valence, even of neutral valence, may have formed. This suggests the formation of a large fraction of the neutral valent $PtCl_4(H_2O)_2^0$ species, seen in the mechanism of Fig. 1. This in turn suggests that the long-term deposition of Pt over alumina in the mid pH range (Fig. 6b) is due to the precipitation of neutral Pt species.

pH Shifts during Adsorption

While potentiometric titration, a technique which calculates surface charge on oxides on the basis of pH shifts, has

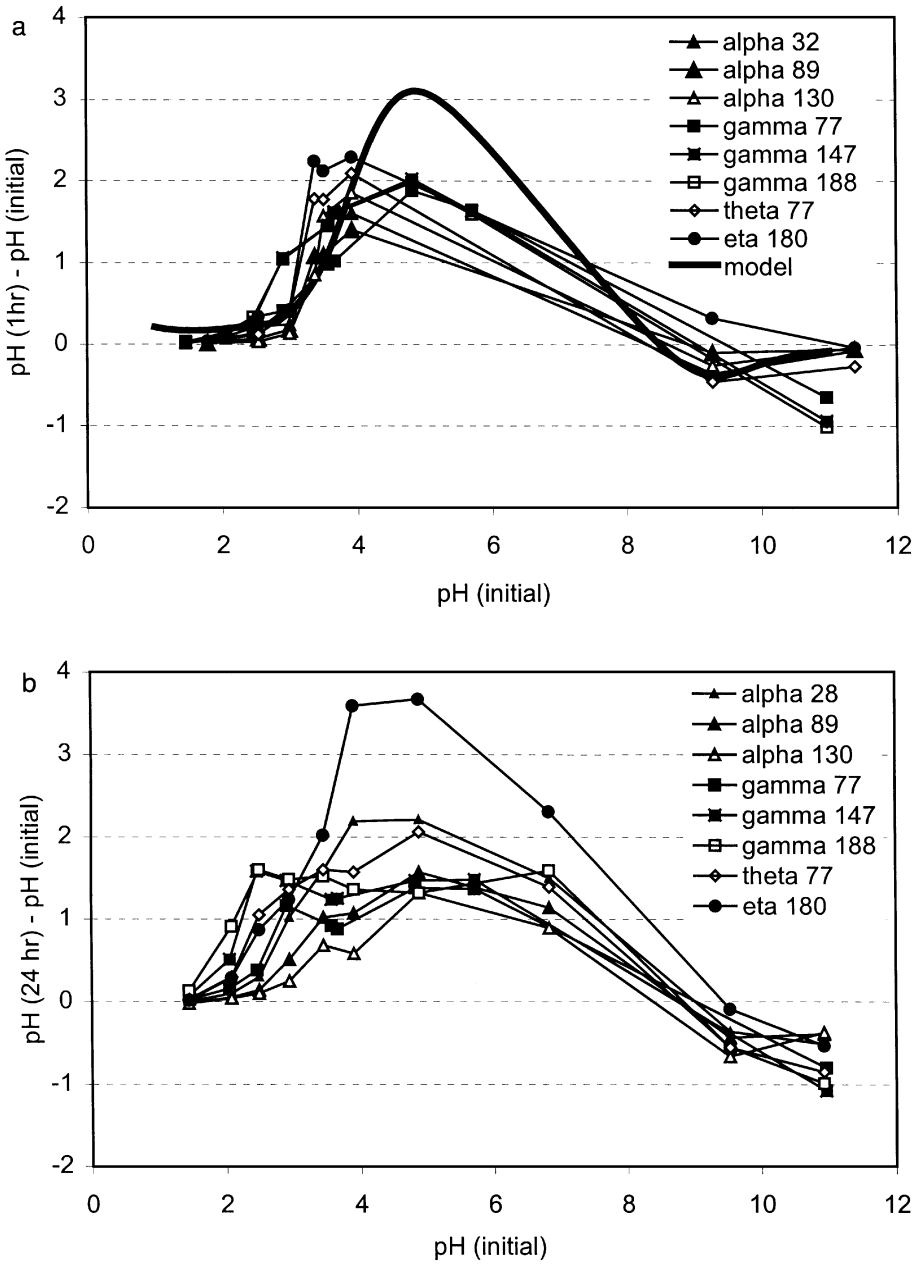

FIG. 7. pH shifts during impregnation over various aluminas versus pH at (a) 1 h (solid line is for RPA model) and (b) 24 h.

been used for many years (14), recognition of the tremendous influence of oxides on solution pH as pertains to catalyst preparation has occurred only more recently, with the demonstration of "mass titration" by Noh and Schwarz (28). A simple non-Nerstian model of surface charging, coupled with a proton balance between the solution and the oxide surface, has enabled the modeling of pH shifts caused by oxides (17). This model accurately simulated the pH shifts caused by alumina reported in the Pt/alumina adsorption study of Mang *et al.* (7). The same model also accurately describes the pH shifts in the PZC determination data of Fig. 2 (17). Model results are included in the pH shift data of Figs. 4a and 7a, using model parameters (hydroxyl density of 8 OH/nm^2 and ΔpK of 5) which were determined independently (12). The fits to both the Pt-free (Fig. 4a) and Pt-containing (Fig. 7a) experiments are reasonable, given that the model contains no adjustable parameters. The effect of CPA is not seen in Fig. 7a, as it appears similar to Fig. 4a. This may arise from a combination of the Pt being adsorbed onto the alumina surface, and the short contact time. Discrepancy in the central pH range is likely due to the effect of CO_2 absorption, also not accounted for in the model for the sake of simplicity. At surface loadings on the order of several thousand m^2/L, the CO_2 effect is minimized

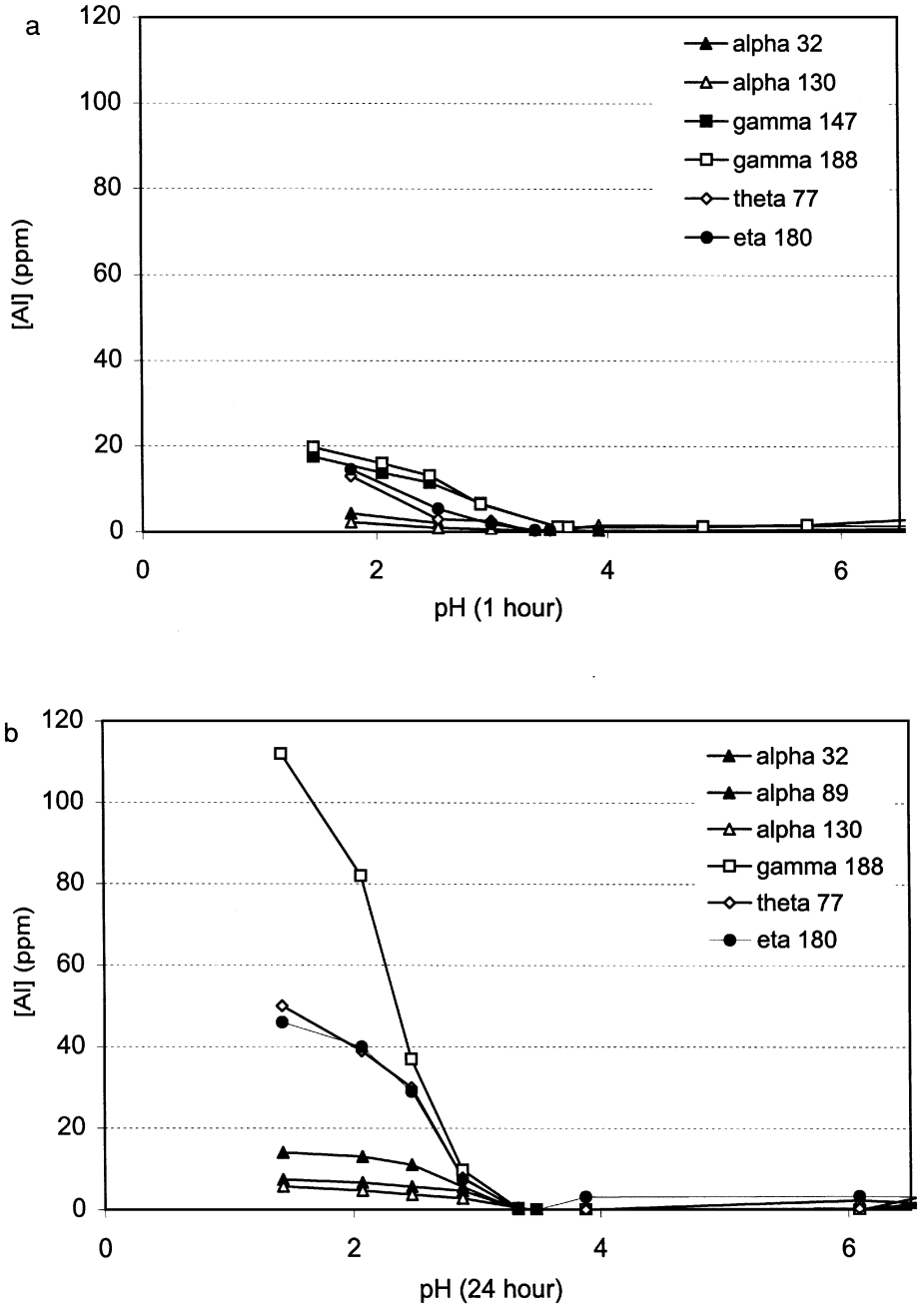

FIG. 8. Dissolved Al from various aluminas versus pH at (a) 1 h and (b) 24 h.

and the discrepancy is much less (17). Also, the low range pH shifts caused by Al dissolution are not accounted for in the model.

In the paper of Mang *et al.*, pH shifts were attributed to adsorption reactions which cause ligand exchange with surface hydroxyl groups (7). The body of evidence in the present work and elsewhere (17, 28) now seems to indicate pH shifts arise simply from the transfer of protons to or from the oxide surface. Other factors consuming or producing protons, such as the metal speciation or aluminum dissolution, might be additive to this phenomenon. These factors might be neglected at short times if they are slow relative to surface protonation/deprotonation.

Discrimination between Adsorption Models

The volcano-type plot of Pt adsorption versus pH has been observed by all other surveys of Pt adsorption over a wide range of pH (3, 7, 9, 10, 12). The reason for the rise in uptake as the pH is lowered from its PZC, in chemical

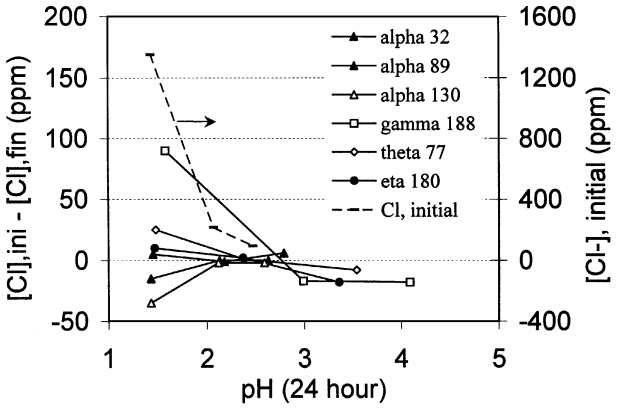

FIG. 9. Cl^- disappearance for various aluminas versus pH 24 h.

and physical adsorption models alike, is that the charge on the alumina surface increases. However, explanations for the retardation at low pH differ. The most recent triple-layer adsorption models proposed for Pt/alumina systems invoke competitive adsorption by chloride (7, 9). Competitive adsorption from Cl^- has also been the classical explanation of why Pt in shell distributions is displaced to the interior of catalyst pellets upon addition of HCl (29). The chloride measurements of Fig. 9 indicate that no chloride is adsorbed, however. Other chemical mechanisms might be postulated which are more consistent with this data, but like the attempt to explain pH shifts with additional adsorption reactions (7), this will necessitate the use of even more adjustable parameters in the chemical adsorption models.

The explanation according to the physical adsorption model is that the increased ionic strength of the more acidic solutions causes an effective decrease in the adsorption equilibrium constant; as opposed to a Cl^--dominated surface, the surface is empty. The explanation of the volcano shape of the Pt uptake curve, according to the RPA model, is shown in Fig. 11. The increase in surface potential as pH is lowered from 8.5 to 3 is seen in Fig. 11a, the increase in ionic strength is shown in Fig. 11b, and the downturn in

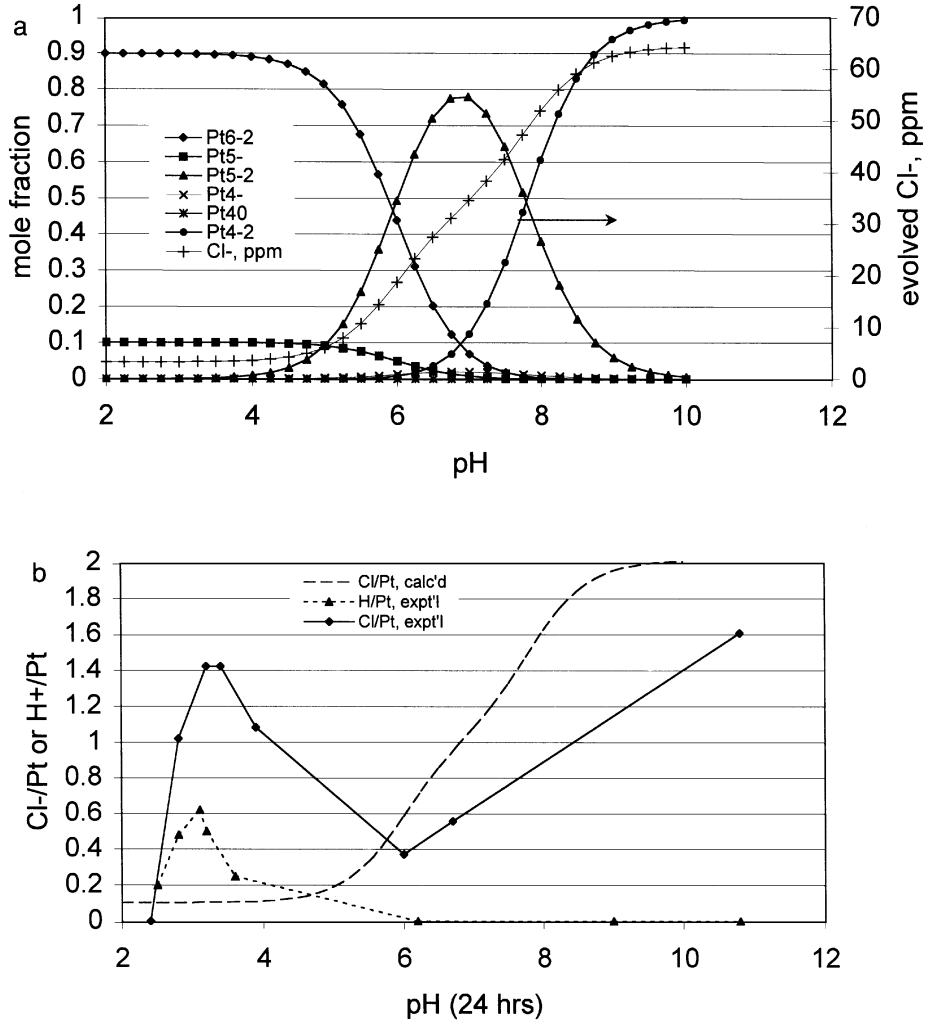

FIG. 10. Speciation of Pt coordination complexes from the reported constants of Sillen and Martell (27).

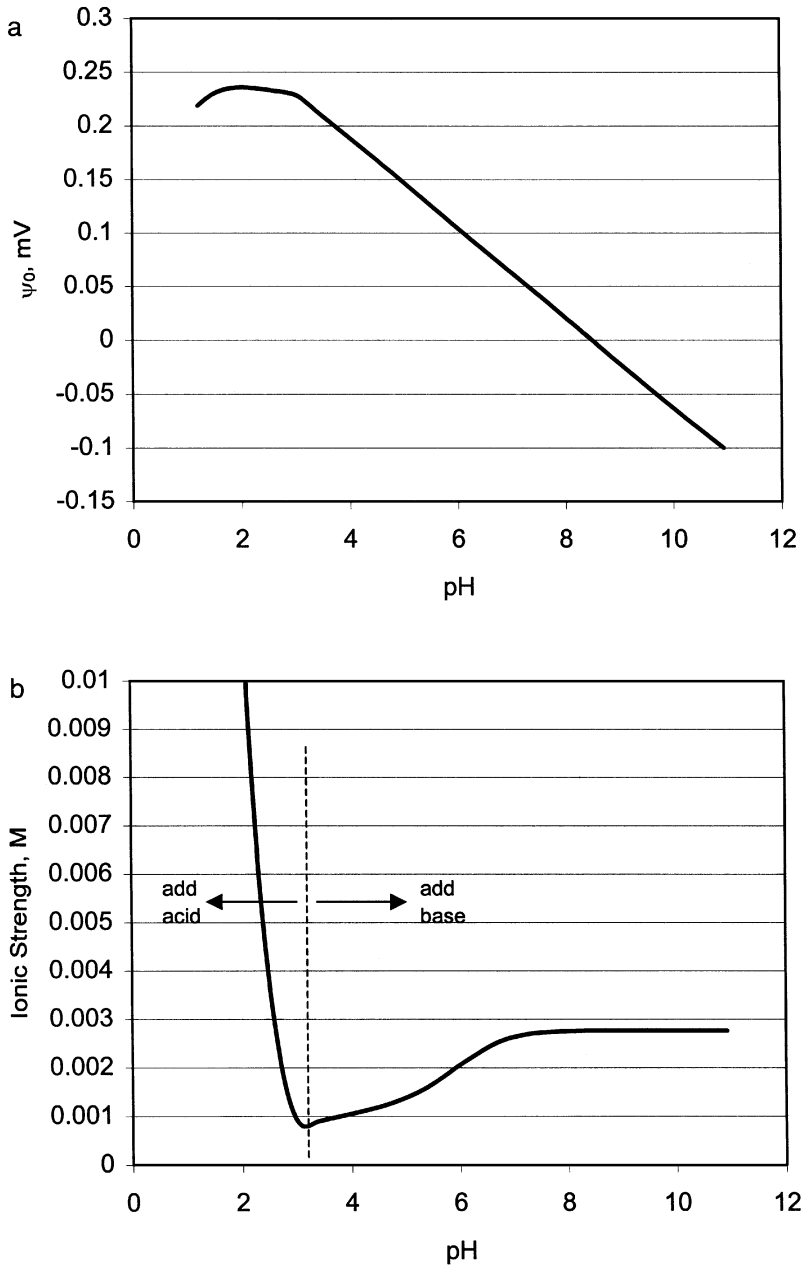

FIG. 11. RPA mechanism of adsorption retardation at low pH. (a) Surface potential versus pH, (b) ionic strength versus pH, and (c) the adsorption equilibrium constant versus pH.

the adsorption equilibrium constant brought about by high ionic strength is shown in Fig. 11c.

According to this theory, the addition of an indifferent electrolyte such as $NaNO_3$, added to the same ionic strength as for HCl, would have the same effect. This was demonstrated in an earlier paper by the current group (10). Schwarz' group demonstrated that the retarding effect was common for a number of 1 : 1, 2 : 1, and 2 : 2 electrolytes (2). Those results, conducted with gamma alumina, have been confirmed for alpha, gamma, and theta phases of alumina by the present group using a number of 1 : 1 electrolytes (30).

Simulations of the experimental Pt uptake data by the revised physical adsorption model (23) are included in Fig. 6. For this calculation, the final pH and not the initial pH was used to best account for the pH shifts due to alumina dissolution and Pt speciation. In contrast to the many adjustable parameters of the chemical model (7), no adjustable parameters are used with the RPA model. The same oxide charging parameters as used for the simulations in Figs. 4a and 7a (8 OH/nm^2, $\Delta pK = 5$), determined from independent measurement, were used here and for Fig. 11. The model agrees reasonably well with the data in the low pH range for both times; at the longer time (Fig. 6b), uptake is

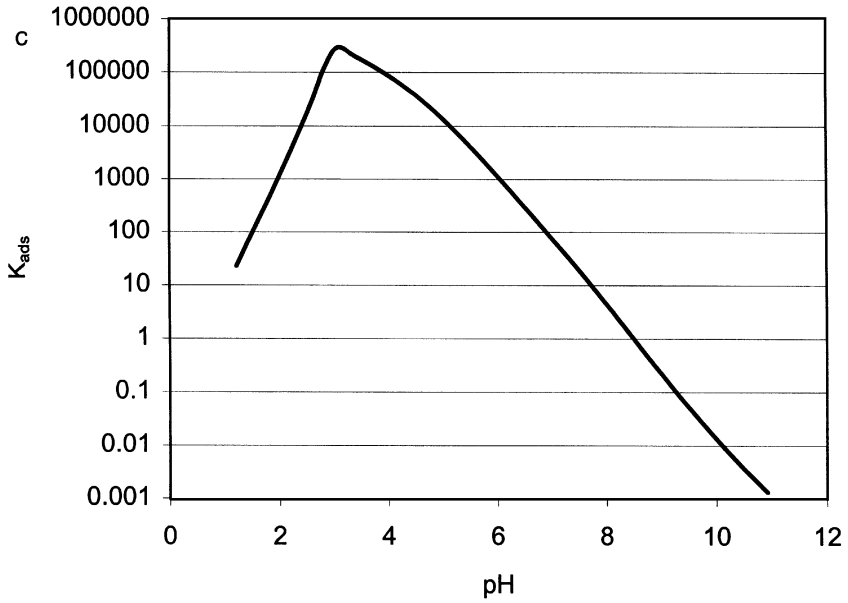

FIG. 11—*Continued*

underestimated by the model in the central pH range. The reason is postulated to be precipitation, indicated earlier, which may be hastened by the presence of a solid surface. With the RPA model, all extant data of Pt uptake on Al_2O_3 have been successfully modeled with this same set of parameters (12).

It is quite noteworthy that Pt uptake over all aluminas can be modeled with a single curve. This is possible since, first, the PZC of all aluminas fall in a narrow range (Fig. 2). Secondly, the hydroxl chemistry of different aluminas should be similar. Severjensky and Sahai have predicted the ΔpK values of oxides based on the inverse of the dielectric constant and the Pauling bond strength of oxide (31, 32). The values of these two quantities are similar for all aluminas. Thirdly, differences in surface area (m^2/g) are compensated by using more mass for the lower surface area material to achieve the same surface loading, 500 m^2/L. On an area basis, then, it appears that all aluminas behave similarly with respect to CPA impregnation. This is precisely as expected from the physical adsorption model, in which the difference between adsorbents is accounted for only by the oxide charging parameters and the surface loading.

A last consideration is directed toward the "coordinative chemical" theory, in which it is hypothesized that Pt can adsorb only after aluminum has dissolved and coordinated to Pt complexes (13, 19). This theory has been postulated for CPA uptake over alumina from a kinetic analysis (19), and from an empirical correlation of Pt uptake to dissolved Al (13). It has been noted previously (11) that the correlation of the latter work was coincidental. The samples with the largest Pt uptake and Al concentration were also the samples with the highest surface area, and in fact if uptake is calculated per surface area, all the different alumina samples exhibited the same Pt adsorption density, about 1.6 μmol Pt/nm^2 (11). In another prior work, the effect of Al dissolution on Pt adsorption was isolated and found to be inconsequential (10).

In the present work the "coordinative chemical" model is disproved since the uptake of Pt is not at all a function of the different types of alumina, which differ widely in solubility. The available surface area is what controls adsorption, and since all experiments were run at the same value of 500 m^2/L, all show the same results.

A further confirmation of the independence of Al dissolution and Pt adsorption can be made by comparing the level of dissolved Al in the absence of CPA to that in the presence of CPA. Data from Figs. 4c and 8c are overlaid in Fig. 12. With the exception of a single point, the two sets

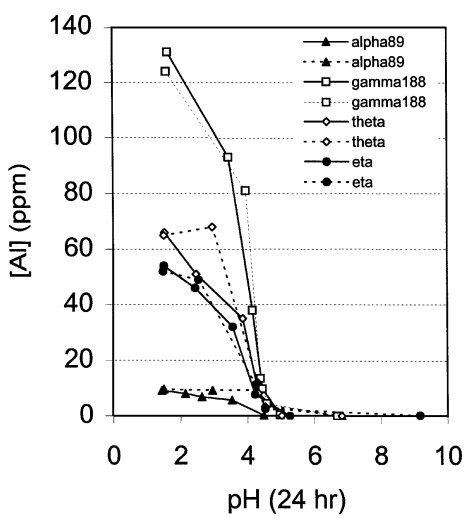

FIG. 12. Comparison of dissolved Al for the Pt-free control and the Pt-containing adsorption experiment.

of data virtually overlap. In further studies of dissolution and adsorption kinetics (not shown) the rate of Al dissolution was seen to be independent of the presence of Pt, and the rate of Pt uptake was independent of the presence of dissolved Al.

ACKNOWLEDGMENTS

The funding of the UOP Research Center, Des Plaines, Illinois, is gratefully acknowledged. J.R.R. is also indebted to the endless efforts of Greg Peterson for the ICP analysis, and to Peter Hennes for instruction on numerous laboratory procedures.

REFERENCES

1. Heise, F. J., and Schwarz, J. A., *J. Coll. Interf. Sci.* **107**, 237 (1985).
2. Heise, F. J., and Schwarz, J. A., *in* "Preparation of Catalysts IV" (B. Delmon, *et al*., Eds.), p. 1. Elvsevier, Amsterdam, 1987.
3. Heise, F. J., and Schwarz, J. A., *J. Coll. Interf. Sci.* **123**, 51 (1988).
4. Heise, F. J., and Schwarz, J. A., *J. Coll. Interf. Sci.* **135**, 461 (1990).
5. Schwarz, J. A., *Catal. Today* **15**, 395 (1992).
6. Contescu, C., and Vass, M. I., *Appl. Catal.* **33**, 259 (1987).
7. Mang, T., *et al*., *Appl. Catal.* **106**, 239 (1993).
8. Papageorgiou, P., *et al*., *J. Catal.* **158**, 439 (1996).
9. Olsbye, U., Wendelbo, R., and Akporiaye, D., *Appl. Catal.* **152**, 127 (1997).
10. Shah, A., and Regalbuto, J. R., *Langmuir* **10**, 500 (1994).
11. Santhanam, N., *et al*., *Catal. Today* **21**, 121 (1994).
12. Regalbuto, J. R., *et al*., *Stud. Surf. Sci. Catal.* **118**, 147 (1998).
13. Xidong, W., *et al*., *Appl. Catal.* **40**, 291 (1988).
14. James, R. O., and Parks, G. A., *Surf. Coll. Sci.* **12**, 119 (1982).
15. Healy, T. W., and White, L. R., *Adv. Coll. Interf. Sci.* **9**, 303 (1978).
16. Parks, G. A., *Chem. Rev.* **65**, 177 (1965).
17. Park, J., and Regalbuto, J. R., *J. Coll. Interf. Sci.* **175**, 239 (1995).
18. Paulhiac, P., and Clause, O., *J. Am. Chem. Soc.* **117**, 11471 (1995).
19. Santacesaria, E., Carra, S., and Adami, I., *Ing. Eng. Chem., Prod. Res. Dev.* **16**, 41 (1977).
20. Karakonstantis, L., Bourikas, K., and Lycourghiotis, A., *J. Catal.* **162**, 295 (1996).
21. James, R. O., and Healy, T. W., *J. Coll. Interf. Sci.* **40**, 65 (1972).
22. Brunelle, J. P., *Pure Appl. Chem.* **50**, 1211 (1978).
23. Agashe, K. B., and Regalbuto, J. R., *J. Coll. Interf. Sci.* **185**, 139 (1997).
24. Wefers, K., and Misra, C., "Alcoa Technical Paper No. 19," Revised, Alcoa Laboratories, 1987.
25. Davidson, C. M., and Jameson, R. F., *Trans. Faraday Soc.* **61**, 2462 (1965).
26. Cox, L. E., and Peters, D. G., *Inorg. Chem.* **8**, 1927 (1970).
27. Sillen, L. G., and Martell, A. E., "The Stability Constants of Metal Ion Complexes," Suppl. No. 1, Special Publication No. 25, The Chemical Society, Burlington House, London, 1971.
28. Noh, J. S., and Schwarz, J. A., *J. Coll. Interf. Sci.* **139**, 139 (1990).
29. Maatman, R. W., *Ind. Eng. Chem.* **49**, 253 (1959).
30. Shadid, S., M.S. thesis, U. Illinois at Chicago, 1998.
31. Sverjensky, D. A., *Geochim. Cosmochim. Acta* **58**, 3123 (1994).
32. Sverjensky, D. A., and Sahai, N., *Geochim. Cosmochim. Acta* **60**, 3773 (1996).